

Benchmarking Unsupervised Online IDS for Masquerade Attacks in CAN

Pablo Moriano^{*†}, *Senior Member, IEEE*, Steven C. Hespeler^{*}, Mingyan Li[‡], Robert A. Bridges[‡]

^{*}Computer Science and Mathematics Division; [‡]Cyber Resilience and Intelligence Division
Oak Ridge National Laboratory, Oak Ridge, TN 37830, USA
{moriano, hespelersc, lim3, bridgesra}@ornl.gov



Abstract— Vehicular controller area networks (CANs) are susceptible to masquerade attacks by malicious adversaries. In masquerade attacks, adversaries silence a targeted ID and then send malicious frames with forged content at the expected timing of benign frames. As masquerade attacks could seriously harm vehicle functionality and are the stealthiest attacks to detect in CAN, recent work has devoted attention to compare frameworks for detecting masquerade attacks in CAN. However, most existing works report offline evaluations using CAN logs already collected using simulations that do not comply with domain's real-time constraints. Here we contribute to advance the state of the art by introducing a benchmark study of four different non-deep learning (DL)-based unsupervised online intrusion detection systems (IDS) for masquerade attacks in CAN. Our approach differs from existing benchmarks in that we analyze the effect of controlling streaming data conditions in a sliding window setting. In doing so, we use realistic masquerade attacks being replayed from the ROAD dataset. We show that although benchmarked IDS are not effective at detecting every attack type, the method that relies on detecting changes at the hierarchical structure of clusters of time series produces the best results at the expense of higher computational overhead. We discuss limitations, open challenges, and how the benchmarked methods can be used for practical unsupervised online CAN IDS for masquerade attacks.

Index Terms—Streaming Data, Online Algorithms, Machine Learning, Anomaly Detection, In-Vehicle Security, CAN Bus

1 INTRODUCTION

TODAY'S vehicles are intricate cyber-physical systems with growing connectivity capabilities to interact with vehicle-to-everything (V2X) technologies [1]–[3]. This increasing connectivity expands the attack surface to adversaries that can access in-vehicle networks. The Controller Area Network (CAN) is the most prevalent protocol used on in-vehicle networks allowing hundreds of electronic control units (ECUs) communicate vehicle functionality [4]–[6]. While the lack of security features makes CAN lightweight and inexpensive, it is susceptible to attacks that aim to manipulate communications and significantly degrade in-vehicle network performance. This has been shown to result in life threatening incidents such as unintended acceleration, brake manipulation, and rogue steering wheel turning [7], [8].

CAN attacks are usually classified as fabrication, suspension, and masquerade attacks [9], [10]. From these, masquerade attacks are the hardest to detect because they do not perturb the regular frame timing which can be detected using time-based methods [11], [12]. Instead, in masquerade attacks, the adversary first silences a targeted ECU and then injects spoofed frames which alters the content of regular frames instead of time-related patterns. This makes masquerade attacks the stealthiest often having an effect on the regular evolution of vehicle states usually measured by sensors [13]. Therefore, recent research efforts have been channeled on designing and deploying intrusion detection systems (IDS) against advanced masquerade attacks in CAN [14]–[17].

IDS for detecting masquerade attacks in CAN are often based on unsupervised anomaly detection techniques aiming to characterize the regular relationships between physical signals in a vehicle [15], [18]. Some of them focus on mining time series relationships based on deep learning (DL) models that consequently have high computational cost [16], [19], [20]. In addition, most of existing CAN IDS approaches are tested offline using datasets or CAN logs already collected from a real or simulated environment. This has been synthesized in existing benchmarking frameworks and comparative studies in the CAN IDS space [18], [21]. The offline evaluation approach is different from online evaluation in that the latter is performed using streaming CAN data from a vehicle, simulation, or data log replay [22]. Therefore, offline evaluation hinders the understanding of realistic capabilities and limitations of CAN IDS in a streaming environment. By benchmarking non DL-based unsupervised online IDS for masquerade attacks in CAN, we seek to provide insights into the effectiveness and limitations of these methods in resource-constrained and streaming environments.

In this paper, we address this gap of knowledge by introducing an empirical and unbiased benchmark of four different non-DL-based unsupervised online IDS for masquerade attacks: Matrix Collocation Distribution, Matrix Correlation Correlation, Ganesan17 [23], and Moriano22 [15]. Here, Matrix Correlation Distribution and Matrix Correlation Correlation methods are simple proposed baselines while Gane-

[†]Corresponding author.

san17 and Moriano22 are already proposed methods in the literature. We test them in simulated masquerade attacks from the ROAD dataset [10]. We rely on a sliding window approach to simulate data log replays of a continuous data stream [24], [25]. We analyze the joint effect of window size and offset on the AUC-ROC as evaluation metric for intrusion detection across the different attacks in the ROAD dataset. We also report an analysis of the testing time per window (TTW) [20] of CAN IDS as a proxy of inference time and discuss insights into the real-time detection capability of these approaches. We further contribute to advance the state of the art in this topic by making publicly available the code of the IDS considered in this study [26]. This furthers research in this topic by allowing other researchers to replicate our results and compare new algorithms with the benchmarked IDS.

Our results indicate that overall the benchmarked unsupervised online CAN IDS are not effective in consistently detecting every attack type in the ROAD dataset. Attacks in the ROAD dataset have different levels of impact on the regular correlation patterns of signals. However, evaluation performance metrics tend to favor Moriano22 and Matrix Correlation Distribution methods. This aligns with the expectation that impacting correlations across signals tends to disrupt the hierarchy of their relationships and their pairwise similarity distribution. Notably, among the variety of attacks in the ROAD dataset, `max_engine_attack` and `correlated_attack` are the ones that can be detected more easily across CAN IDS. Our results also shed light on the impact that sliding window parameters (i.e., window length and offset) have on the detection task. Overall, across methods and attack types, we identify conditions that make certain algorithms more suitable to operate in a real-time detection environment.

2 BACKGROUND

2.1 CAN Protocol

CAN is a message-based communication standard for interconnecting ECUs within industrial application and vehicles. Developed by Bosch in 1980s, CAN operates at Open Systems Connection (OSI) lowest two layers (physical and data-link layers), and is renowned for its reliability and efficiency in automotive and industrial networking applications. CAN facilitates communication among ECUs without requiring a central bus controller, using two-wire bus for seamless message transmission through frames containing arbitration, control, data, and error-checking fields, as illustrated in Fig. 1. Of particular relevance to this paper’s context are two fields, the 11-bit Arbitration ID and the up-to-8-byte data field.

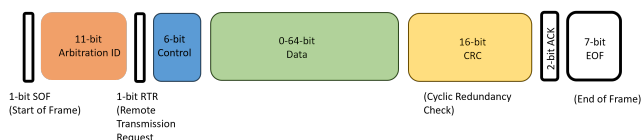


Fig. 1. CAN frame illustration.

The arbitration ID serves as a unique identifier for messages transmitted over the bus. This ID is crucial for

distinguishing between different messages and plays a key role in determining message priority. Lower ID values indicate higher message priority, allowing critical messages to be sent without delay. The data field contains the actual information being transmitted between ECUs. The payload consists of up to 8 bytes of data. Each or multiple bytes represent a specific piece of information, known as “signal”, such as sensor readings or status information. The data payload is essential for exchanging real-time data between ECUs. CAN frames with a certain arbitration ID are transmitted at a predetermined frequency with fixed payload structure. For instance, the power control module transmits ID 0x102 with data field containing engine RPM, vehicle speed, and odometer signals every 0.05s [10].

CAN also includes a built-in sophisticated fault confinement mechanism to handle anomalies such as faulty cables, noise, or malfunctioning CAN nodes etc. Each node constantly monitors its performance and creates an “error frame” in response to detecting a CAN error. There are three possible CAN error states: error active state, error passive state, and error bus-off state, with the last one being prohibited from sending or receiving CAN messages. Prior work by Cho and Shin [27] provides more details on CAN error handling.

2.2 CAN Vulnerabilities

Despite being robust, the CAN protocol can suffer from a multitude of cyber attacks due to its inherent vulnerabilities. Firstly, the absence of communication encryption protection leaves CAN messages susceptible to interception and manipulation, allowing the attackers to eavesdrop on communications or tap into and alter the network communication without being detected. Secondly, the lack of authentication mechanisms implies that nodes within the CAN network cannot verify the identities of message senders, making it easier for the unauthorized parties to gain access and tamper with transmission data. Moreover, the broadcasting nature of the CAN protocol, notably when compounded by lack of encryption and authentication, essentially allows any node to receive messages intended for others, and to inject illegitimate messages at its will. By exploiting such vulnerabilities, a malicious node can potentially manipulate message arbitration ID to disrupt message delivery priorities, launch Denial of Service (DOS), or launch impersonation attacks, to create communication errors or system malfunctions. Finally, CAN vulnerabilities can also lead to exploits of higher-level protocols. An example would be an attack on ECUs’ Unified Diagnostic Services (UDS)—a diagnostic communication protocol used within automotive electronics, by injecting and manipulating CAN messages [28].

In terms of attacks that manipulate CAN messages, there are three categories of exploits:

- *Fabrication attacks*, employs a compromised ECU to inject messages with malicious IDs and data fields. Typically CAN IDs are deliberately set to low values, signifying high priority. Continuously injecting such high-priority messages can eventually disrupt legitimate ECUs from transmitting theirs leading to DoS-type attacks or targeting vehicle functions.

- *Suspension attacks*, where the adversary seeks to compromise an ECU to prevent it from transmitting some or all of its messages. This could be achieved by removing an ID frame(s) to disconnect the ECU from the CAN bus, thereby halting the transmission of corresponding signal values.
- *Masquerade attacks*, the most sophisticated category, involve the adversary initially suspending messages from a specific ID of a targeted ECU, then spoofing messages using this ID at a realistic frequency, thus effectively masquerading as the compromised ECU.

3 RELATED WORK

Here we review and contrast previous offline benchmark studies on CAN IDS (Section 3.1) and online CAN IDS methods (Section 3.2).

3.1 Prior Work Closely Related to the Present Study

Ji et al. [21] presented a comparative analysis of four statistical-based CAN IDSes using entropy, clock skew, ID sequences, and CAN bus throughput. Benchmarked methods relied only on ID timestamp arrivals. Their evaluation was done in simulated attack datasets. They found that the clock skew method performed best across attacks while the entropy method falls short on detecting replay attacks.

Dupont et al. [29] introduced a unifying framework for CAN IDS evaluation of time-based methods. In doing so, they used data from two live vehicles and a CAN prototype. They used both simulated attacks and publicly available datasets with attacks [30]. They found that among compared methods, they perform well only on attacks that generate significant disruptions in CAN traffic. They suggested that methods that consume bit representations and semantics of CAN messages will perform better.

Stachowski et al. [31] introduced a framework for benchmarking CAN IDS. Their approach focused on the online evaluation of three existing solutions from identified vendors, so that CAN IDS are tested in real vehicles for real-time intrusion detection. Targeted ID attacks were introduced in test vehicles while vehicles were in motion and stationary. None of the tested CAN IDS was found effective for detecting the variety of attacks.

Blevins et al. [32] focused on benchmarking time-based CAN IDS on the fuzzy and targeted ID attacks from the ROAD dataset. Benchmarked methods include mean inter-message time, fitting a Gaussian curve, kernel density estimation, and binning. They found that the binning method outperformed the other methods, specially those fitting a distribution on inter-arrival times, in terms on AUC-ROC, AUC-PR, and F1 score. They reported a latency analysis for the binning algorithm.

Agbaje et al. [33] introduced a framework for comprehensive performance evaluation analysis of eight state-of-the-art CAN IDS. The proposed framework provides a consistent methodology to evaluate and assess CAN IDS. They focus on using previously published datasets recorded from a real vehicle and report traditional classifier performance evaluation metrics to reduce uncertainty when comparing IDS approaches from different sources.

Pollicino et al. [34] introduced an experimental comparison on the performance evaluation of eight CAN IDS algorithms over two different datasets, an in-house one and one that is already publicly available (i.e., OTIDS [30]). The algorithms they benchmarked consume only time-based information from CAN frames as they are intended for detection of fabrication attacks. They open-sourced code implementations of these algorithms to allow reproducibility of research results and detail an unbiased experimental comparison.

Sharmin et al. [18] reported results of a comparative evaluation of four statistical and two ML-based CAN IDS in the ROAD dataset, including masquerade attacks. In addition to reporting traditional evaluation metrics such as accuracy, precision, recall, and F1 score, they included balanced accuracy, informedness, markedness, and Matthews correlation coefficient (MCC) which are better suited for handling imbalanced datasets [35]. They also reported training and testing time for each IDS. They found that frequency-based approaches generally perform well at detecting fabrication attacks while other algorithm categories did not perform well based on low MCC scores.

Compared to the benchmark studies mentioned above, the present paper is unique because it focuses on online IDS methods for masquerade attacks. Note that previous benchmark studies focused on: (1) comparing CAN IDS methods in an offline fashion (see works [18], [21], [29], [32], [34]); and (2) performing evaluation tests only on fabrication attacks (see works [21], [29], [31]–[34]). By benchmarking CAN IDS methods on these two key aspects, we contribute to fill this gap of knowledge by analyzing the performance of unsupervised online CAN IDS in online fashion and testing them on the most stealthy CAN bus attacks, i.e., masquerade attacks. Our contribution enriches the state of the art by introducing a more realistic assessment of CAN IDS behavior in a realistic but constrained environment.

3.2 Other Prior Work Related to the Present Study

Desta et al. [36] proposed a CAN IDS based on a LSTM sequence predictor model focused on predicting ID sequences. They performed in-house collection of CAN data using a real car. They replayed a CAN data log using the socketCAN API to evaluate their CAN IDS. They found that they can obtain better results by using the log loss of the predicted ID and the true ID.

Sunny et al. [37] proposed a hybrid CAN IDS that leverages patterns of recurring messages and time interval between them. The proposed approach produces fast inference times being informed by best and worse time intervals between two consecutive frames. As CAN messages are expected to be published every 2 ms, they conclude that the proposed method can be used for real-time settings on simulated attack scenarios.

Jedh et al. [38] evaluated four architecture designs for real-time CAN IDS under malicious speed reading message injections. They focus on a single ML-based IDS that captures the pattern of the sequences of CAN messages represented with a direct graph. They showed that the optimal architecture for deployment a real-time CAN IDS is based on two processes, a process for CAN monitoring and another one exclusively for anomaly detection.

Jadidbonab et al. [39] introduced an automotive security testbed that combines a full-scale in-vehicle network (i.e., vector CANoe) and a car simulator (i.e., CARLA) to generate network traffic in realistic scenarios. They tested ML-based IDS on their testbed and found that online algorithms performed poorer when compared to training offline classifiers on previously collected logs.

4 METHODS

Common to all the methods benchmarked in this work is our focus on processing a set of time series representing signals in the CAN bus. For that, we assume that we have access to the time series representation obtained from CAN logs captured during a vehicle’s drive. Recall that the subsequent methods are expected to work in online fashion. This means that they process a time series stream to provide near real-time alerts.

Note that although streaming and online algorithms are often used as synonyms, here we make the distinction between these two and point out that streaming algorithms process each point as soon as it is received, while online algorithms process small batches at a time [25], [40], [41]. In our work, we use the latter definition, when we refer to online algorithms, i.e., algorithms that repeatedly process small parts of a continuous time series stream. Note that our inclination to benchmark unsupervised learning methods is guided in part by the fact that it is challenging to apply supervised methods on streaming data due to their static nature [42].

4.1 Threat Model

We assume a scenario where an adversary has already gained access to the CAN bus (e.g., by the OBD-II port or through wireless communication) [43]. Here, the adversary compromises two ECUs, one as a strong attacker (i.e., fully compromising an ECU including capabilities for injecting arbitrary attack messages) and the other as a weak attacker (i.e., being able to stop/suspend the ECU from transmitting certain messages) [9].

4.2 Time Windows

The presented benchmark is based on sliding time windows of the stream of time series data. The assumption behind using windows is that more recent information is more relevant for decision-making than past data. In particular, we focus on using *sliding windows* of fixed size for anomaly detection [44]. The windows are defined in terms of the number of observations or sequence-based windows [24]. This involves a sequence of ω -length windows (i.e., $\omega \in \mathbb{Z}$) $W = \{W_j : j \geq 1\}$ with a sliding step (or offset $\delta \in [1, \omega]$) and observations arriving sequentially. Let Y_t for $t \geq 0$ be a set of time series in a given window W , then Y_t contains time series over the interval $[\delta \times (j-1), \delta \times (j-1) + \omega]$. Hence, Y_t is a set of time series of the most recent ω observations up to time t with δ observations that expire. Figure 2 shows this concept visually.

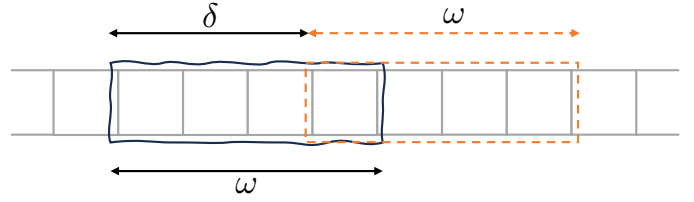


Fig. 2. Sliding windows concept. The stream of time series data is partitioned using windows of length ω . The sliding windows step, or offset, is δ .

4.3 Experimental Design

Here we describe our proposed benchmarking framework. More details can be found in Fig. 3. Our proposed framework has two phases: i) P_1 : training phase and ii) P_2 : testing phase. These phases have some sequential tasks. Some of them are unique to one phase while others are common to both phases. The tasks are: i) T_1 : data collection and preprocessing, T_2 : model fitting, and T_3 : model testing. P_1 consists of tasks T_1 and T_2 , whereas P_2 consists of tasks T_1 , T_2 , and T_3 .

The proposed benchmark framework uses time windows for data processing and attack detection within the same time window. This means that our benchmark is focused on detecting attacks at the window level rather than at the message level. Note that both phases are considered to be accomplished in a light-weight device (e.g., Raspberry Pi or Nvidia Jetson Nano). We now explain the technical aspects of the framework in more detail.

4.3.1 Training Phase (P_1):

1) Data Collection and Preprocessing (T_1):

The first task common to all the algorithms in our benchmark is the configuration of the data collection and preprocessing pipeline. We assume that the benchmarked algorithms run on light-weight devices connected to the CAN bus through the OBD-II port or a dedicated ECU with direct access to the CAN bus. This setup allows continuous collection of raw CAN messages along with its translation from binary to time series using its corresponding decoding instructions. Note that there are available open-source CAN data loggers such as SavvyCAN and SocketCAN and commercial tools such as CANalyzer and VehicleSpy. We also assume that for translating CAN binary payloads to multi-dimensional time series, algorithms are loaded with OEM’s DBC file or use CAN decoding software such as LibreCAN, CAN-D, or CANMatch [45]–[47]. For a more comprehensive discussion on CAN signals reverse engineering, we refer the reader to the survey by Buscemi et al. [3].

We focus on processing a set of n signals, i.e., $\mathcal{S} = \{s_1, s_2, \dots, s_n\}$. Here n means the total number of decoded signals. As each of these time series is generated at a characteristic frequency (imposed by their corresponding ID), we linearly interpolated them in common timesteps to have the same frequency producing evenly spaced time series. We use a common frequency of 100Hz to take into account the fact that most IDs do not send messages above this frequency threshold. This ensures that $\forall s_i \in \mathcal{S}, |s_i| = t_0$, where t_0 is the total number of time steps in the training set.

This multivariate time series data is stored in a matrix $\mathbf{X}_{train} \in \mathbb{R}^{t_0 \times n}$. On this matrix, we discard any constant time series and apply min-max normalization to the remaining time series.

2) Model Fitting (T2):

We fit data-driven models for each of the benchmarked methods using the training data, i.e., \mathbf{X}_{train} . Fitted models in this task are then used as the regular (normal) state representation from which we derive comparisons with models fitted at the testing stage. The details of the fitted models for each of the benchmarked methods are in Section 4.4.

4.3.2 Testing Phase (P2):

The testing phase executes similar tasks as already discussed in the training phase (see tasks T1 and T2 in Section 4.3.1) and adds T3. Note that while P1 is run only once, the tasks in P2 are run continuously and sequentially as new messages are processed and there is a need to check for anomalies. We detail here changes with respect to specific parameters.

1) Data Collection and Preprocessing (T1):

In the testing stage, data is processed using a sliding window approach (see more details in Section 4.2). Specifically, smaller sections of \mathbf{X}_{test} of length ω are selected to create a view of the streaming ($\in \mathbb{R}^{\omega \times n}$). Benchmark methods consume this batch of data to arrive at conclusions.

2) Model Fitting (T2):

We fit the benchmarked methods with their specific models on \mathbf{X}_{test} . The specifics of the fitted models are discussed in Section 4.4.

3) Model Testing (T3):

This step entails a data-driven decision-making for deciding if a particular window is containing an anomaly or not. The specifics of the criteria for detection are discussed in Section 4.4.

4.4 Benchmarked Algorithms

This subsection describes in detail each of the four algorithms used in this research. For the sake of readability, we associate each algorithm name of the first author and the last two digits of the publication year (when applicable). Specifically, we describe the following methods: Matrix Correlation

Distribution (see Section 4.4.1), Matrix Correlation Correlation (see Section 4.4.2), Ganesan17 [23] (see Section 4.4.3), and Moriano22 [15] (see Section 4.4.4).

We notice that none of the benchmarked algorithms has been distributed with a corresponding implementation. In addition, many of their implementation details are not provided. To address these limitations, we make available our referenced implementations and provide a detailed description of the assumptions and parameters tested in each of the algorithms. This allows practitioners in the area the opportunity to easily replicate our experiments and benchmark novel signal-based detection algorithms with respect to the state of the art. Note that benchmarked algorithms produce anomaly scores in the range 0 to 1 that is being used for computing evaluation metrics.

All method computes pairwise Pearson correlations among time series in \mathbf{X}_{train} (and \mathbf{X}_{test}) obtaining $\mathbf{R}_{train} \in \mathbb{R}^{n \times n}$ (and corresponding $\mathbf{R}_{test} \in \mathbb{R}^{n \times n}$), symmetric matrices whose r_{ij} entry is the Pearson correlation coefficient [48] between the signals s_i and s_j . Pearson correlation values that are close to ± 1.0 indicate strong positive or negative correlation. Note that time series that have positive correlations are expected to move jointly (i.e., when one time series increases or decreases, the other time series also increases or decreases). As vehicle dynamics are constrained by laws of nature, we expect that: (1) clusters of correlated signals emerge, for example, as there is an increase in the speed of the vehicle, there is a subsequent increase in the speedometer reading and the speed of the four wheels, and (2) such clusters are disturbed upon a cyberattack given that time series correlations could be broken or changed significantly.

We let \mathbf{U} denote the strictly upper triangular matrix of \mathbf{R} , i.e., $u_{ij} = r_{ij}$ if $i < j$ and $u_{ij} = 0$ if $i \geq j$. We create strictly upper triangular matrices \mathbf{U}_{train} , \mathbf{U}_{test} , respectively, for both training and testing correlation matrices (\mathbf{R}_{train} and \mathbf{R}_{test}) to estimate pairwise similarity distributions among time series.

4.4.1 Implementation of Matrix Correlation Distribution

This method seeks statistical significance of the signals' pairwise Pearson correlations. Using \mathbf{U}_{train} , \mathbf{U}_{test} as above,

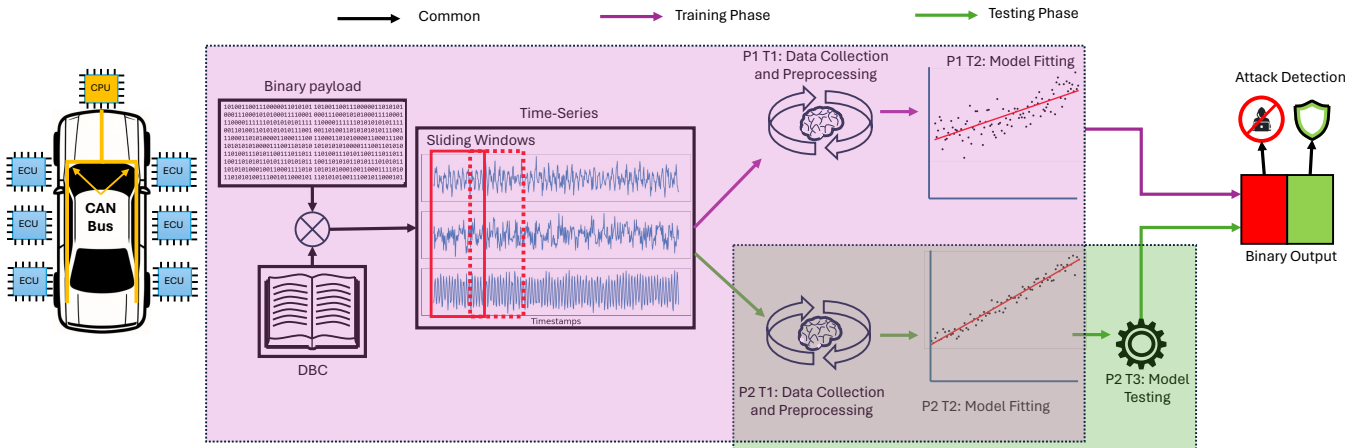


Fig. 3. An overview of our proposed benchmark framework.

we use the Mann-Whitney U test [49] p -value to create an anomaly probability score; specifically, one minus the p -value is the anomaly score so that a larger score is more anomalous. The Mann-Whitney U test is a non-parametric test often used to test the difference in location between distributions. As the Mann-Whitney U test null hypothesis is that the Pearson similarity distribution underlying benign conditions and attack conditions is the same, we use one minus the p -value as the anomaly score. Intuitively, higher p -values suggest not rejecting the null hypothesis; this translates to a lower anomaly probability score. Conversely, lower p -values suggest rejecting the null hypothesis; this translates to a higher anomaly probability score.

4.4.2 Implementation of Matrix Correlation Correlation

This method considers the upper triangular entries of $\mathbf{U}_{train}, \mathbf{U}_{test}$ (the signals' pairwise Pearson correlation coefficients) and computes the statistical significance of their Spearman correlation [50], a measure in $[-1, 1]$ of their members ordinal rank. Simply unravel the upper triangular entries of $\mathbf{U}_{train}, \mathbf{U}_{test}$ into two sequences and compute their Spearman correlation. Note that Spearman correlation furnishes, alongside the correlation value, a p -value giving the likelihood that the two input vectors are from uncorrelated systems (so low p -value corresponds to the two input vectors coming from correlated systems). We focus on the p -value of the Spearman correlation as this captures the reliability of the correlation. The Spearman correlation coefficient is better suited for non-normally distributed continuous data, ordinal data, or data with potential outliers as a measure of monotonic association [51]. Pearson correlation is also scaled in the range ± 1 indicating a constantly increasing or decreasing monotonic association while 0 indicating no monotonic association. The Spearman correlation null hypothesis is that there is no correlation between the strictly upper triangular correlations in training and testing (opposite to the first test above); hence, we use the p -value as the probability score. Here, higher p -values suggest not rejecting the null hypothesis; this translates to a higher anomaly score. Conversely, lower p -values suggest rejecting the null hypothesis; this translates to a lower anomaly score.

4.4.3 Implementation of Ganesan17

This method focuses on computing clusters of time series defining a context (such as aggressive or sudden driving). Note that this method does not rely on cluster characterization during training and only relies on processing testing windows. Specifically, for each time window of length ω , the DBSCAN clustering method [52] is applied to a distance matrix $\mathbf{D}_{test} \in \mathbb{R}^{n \times n}$ computed as $2 * (1 - \mathbf{R}_{test})$, i.e., a squared Euclidean distance to identify clusters [53]. DBSCAN is a density-based non-parametric clustering algorithm that works by grouping points with many nearby neighbors and marking as outliers the points that lie alone in low-density regions. By analyzing clusters of time series as opposed to individual pairs, this method aims to capture richer relationships between signals. We used the same parameter values used in Ganesan et al. [23], namely $eps = 1$ capturing how close points should be to each other to be considered part of a cluster and $min_samples = 1$ capturing the minimum number of points to form a dense region.

For detection, once clusters of time series have been identified, pairwise cross correlations among time series within clusters are computed and compared with those expected for that cluster. Specifically, for each correlation pair, the deviation from the mean correlation value for that cluster is computed. Among each possible pairs, the maximum deviation (or error) is extracted and compared in terms of the number of standard deviations from the mean. Among all the errors in a single cluster, only the maximum error among clusters is used as reference. Finally, among all the errors among clusters, the probability of being anomalous is estimated based on the normal distribution approximation of maximum errors evaluated at a particular error, i.e., the probability that the distribution of maximum errors will take a value less or equal than the error.

4.4.4 Implementation of Moriano22

This method focuses on computing the similarity of hierarchical clusterings of time series in training and testing. Specifically, pairwise correlations matrices \mathbf{R}_{train} and \mathbf{R}_{test} are used to feed an agglomerative hierarchical clustering (AHC) algorithm [54]. We used a Ward's linkage as a metric for dissimilarity between clusters as it maximizes detection results as in the original paper [15]. The output of the AHC is a hierarchical clustering or a hierarchy of clusters (i.e., a set of nested clusters that are organized in a tree-like diagram known as dendrogram).

For detection, in each time window of length ω , we compute the clustering similarity s between the hierarchical clustering from training (computed once) and the hierarchical clustering computed during that specific time window. Here, similarity is used as a proxy of the distance between both hierarchical clusterings. We compute the similarity between hierarchical clustering using the CluSim method [55] based on the work by Gates et al. [56]. We parametrized CluSim by letting $r = -5.0$ and $\alpha = 0.9$. Here, r is a scaling parameter that defines the relative importance of memberships at different levels of the hierarchy. That is, the larger r , the more emphasis on comparing lower levels of the dendrogram (zoom in). In addition, α is a parameter that controls the influence of hierarchical clusterings with shared lineages. That is, the larger α , the further the process will explore from the focus data element, so more of the cluster structure is taken into account into the comparison. The similarity value provided by this method, s , lies in the range $[0, 1]$, where 0 implies maximally dissimilar clusters, and 1 corresponds to identical clusters. Therefore, we report the anomaly score (or probability of detection) as $1 - s$.

4.5 Dataset

We ran the proposed benchmark on the ROAD dataset [10]. The ROAD dataset is a publicly available dataset for CAN IDS that contains benign and attack CAN data collected from a real vehicle. An important feature of ROAD is that it provides samples of masquerade attacks which are the types of attacks we are interested in detecting with the bechmarked methods. Note that masquerade attacks in ROAD are identical to the corresponding targeted ID captures but with the ambient frames of the targeted ID removed during the attack period to simulate the masquerade attack. The

TABLE 1
CAN captures used from the ROAD dataset [10].

	Description	# Files	Used	Duration (min)
Training	Dynamometer Various Ambient	10	✓	108.2
	Road Various Ambient	2	✓	70.6
	<i>Total</i>	12	12	178.8
	Correlated Signal Fabrication Attack	3	✗	1.3
Testing	Correlated Signal Masquerade Attack	3	✓	1.3
	Fuzzing Fabrication Attack	3	✗	0.7
	Max Engine Coolant Temp Fabrication Attack	1	✗	0.4
	Max Engine Coolant Temp Masquerade Attack	1	✓	0.4
	Max Speedometer Fabrication Attack	3	✗	3.9
	Max Speedometer Masquerade Attack	3	✓	3.9
	Reverse Light Off Fabrication Attack	3	✗	2.1
	Reverse Light Off Masquerade Attack	3	✓	2.1
	Reverse Light On Fabrication Attack	3	✗	3.2
	Reverse Light On Masquerade Attack	3	✓	3.2
	Accelerator Attack (In Drive)	2	✗	2.7
	Accelerator Attack (In Reverse)	2	✗	3.2
	<i>Total</i>	33	13	10.9

ROAD dataset also provides already translated CAN time series from log files. By using ROAD in this study, we ensure comparing the performance of proposed methods with realistic, verified, and labelled attacks as opposed to synthetic ones. This allows performing the comparison under realistic conditions.

We report results on the proposed benchmark in each of the masquerade attacks provided in the ROAD dataset. Note that each of the masquerade attack files in ROAD contains hundreds of time series coming from hundreds IDs each of them with up to a few dozen signals. Table 1 shows the specific files we used from ROAD. In particular, we used the following attacks in increasing level of detection difficulty: correlated signal, max speedometer, max engine coolant temperature, reverse light on, and reverse light off. In the correlated signal attack, the correlation of the four wheel speed values is manipulated by changing their individual values. In the max speedometer and max engine coolant attacks, the speedometer and coolant temperature values are changed to their maximum. In the reverse light attacks, the state of the reverse light is modified so that it does not match the current gear of the vehicle (i.e., reverse light is off when the vehicle is in reverse and the reverse light is on when the vehicle is in forward gear).

We used the longest benign capture (i.e., `ambient-highway-street-driving-long`) for learning the normal state of the system (≈ 1 hour of data). We use all the available attack data in the masquerade category, i.e., three files in the correlated attack category (≈ 1.3 minutes), three files in max speedometer attack category (≈ 3.9 minutes), one file for the max engine coolant attack category (≈ 0.4 minutes), three files for reverse light on attack category (≈ 3.2 minutes), and three files for the reverse light off attack category (≈ 2.1 minutes).

4.6 Evaluation Metrics

This study focuses on comparing the detection capability of the benchmarked algorithms on the ROAD dataset. As such, we report summarized results over a range of detection thresholds and focus on the area under the receiver operating characteristic curve (AUC-ROC) metric. The AUC-ROC reflects the overall performance of the benchmarked algorithms based on the variation of the true positive rate

(TPR) with respect to the false positive rate (FPR) at various thresholds [57]. Mathematically, it is expressed as

$$\text{AUC-ROC} = \int_0^1 \text{TPR}(\text{FPR}^{-1}(x)) dx.$$

AUC-ROC takes values in the interval $[0, 1]$. In particular, an algorithm whose predictions are 100% wrong has an AUC-ROC of 0.00; while an algorithm whose predictions are 100% correct has AUC-ROC of 1.00. A reasonable way of interpreting AUC-ROC is as the probability that the detection algorithm ranks a random positive window more highly than a random negative window, which is desirable in our case. Note that although the AUC-ROC provides an overly estimated view in highly imbalance datasets [58], we stick to AUC-ROC as the proportion of time windows overlapping with attack intervals is not imbalanced (i.e., for most of the window length and offset combinations is above 40%).

4.7 Performance Metrics

For assessing the real-time capabilities of the benchmarked algorithms, we also report the latency that these methods have to infer detection decisions on the sliding windows being processed. In doing so, we report the testing time per window (TTW), for each combination of window length (ω) and offset (δ), following the concept of testing time per packet used by Nichelini et al. [20]. We define TTW as

$$\text{TTW} = \frac{\text{Total Detection Time}}{\text{Number of Windows}}$$

Our experiments were conducted on a AMD EPYC 7702 64-Core Processor Central Processing Unit (CPU), 256 GB of RAM, running Ubuntu 22.04.4 LTS (Jammy Jellyfish). TTW provides a way to estimate the applicability of the benchmarked algorithms in a real-time setting.

5 RESULTS

In this section, we detail the experimental evaluation of the benchmarked algorithms on the ROAD dataset. All methods were implemented in Python 3.8.12. We use the `sklearn.metrics` module to compute the evaluation metrics and the `timeit` module to compute the TTW of each benchmarked algorithm. To enable the reproducibility of the benchmarked methods, we make the code available in GitHub.¹ We conduct three different but complementary analysis.

First, we compute and contrast the detection performance (based on AUC-ROC) of each algorithm per attack category in the ROAD dataset. In doing so, we display heatmaps (Section 5.1). We hypothesize that each algorithm is better suited for detecting specific attacks in the ROAD dataset and that there is a range of (ω, δ) combinations that maximizes AUC-ROC.

Second, we summarize evaluation metrics using summary statistics derived from the heatmaps (Section 5.2). Specifically, we report the mean (μ), standard deviation

¹<https://github.com/pmoriano/benchmarking-unsupervised-online-IDS-masquerade-attacks>

(σ), median (η), minimum (min), including the combination of window length and offset that produces it, and maximum (max), including the combination of window length and offset that produces it. This analysis supports our hypothesis that there are better suited detection algorithms for each attack category. Overall, Moriano22 detection algorithm produces, on average, the best detection performance among attacks in the ROAD dataset. In contrast, Ganesan17 detection algorithm produces the worst detection performance among attacks in the ROAD dataset. Furthermore, we found that the easiest attacks to detect are the `max_engine_coolant_attack` and `correlated_attack`. Furthermore, we find that the `max_speedometer_attack` and `light_on_attack` are the hardest to detect.

Lastly, we summarize TTW as a proxy of performance (Section 5.3). In particular, we report the mean (μ), standard deviation (σ), median (η), minimum (min), including the combination of window length and offset that produces it, and maximum (max), including the combination of window length and offset that produces it. This analysis reveals that more sophisticated algorithms (e.g., Ganesan17 and Moriano22) incur performance overhead for producing better detection evaluation metrics. Overall, Matrix Correlation Distribution produces, on average, the quickest TTW among attacks in the ROAD dataset. In contrast, Moriano22 detection algorithm is at least $4\times$ slower. It is worth noting that detection algorithms that run faster (i.e., Matrix Correlation Distribution and Matrix Correlation Correlation) perform even better than Ganesan17 (see Table 3). We did not found significant differences on TTW per attack categories.

5.1 Evaluation Metrics Contrast

Figs. 4, 5, 6, 7 show the detection performance of each detection algorithm (i.e., Matrix Correlation Distribution, Matrix Correlation Correlation, Ganesan17, and Moriano22, respectively). Each cell in the heatmaps depicts a single AUC-ROC value for a specific combination of ω and δ . Note that attack types are displayed horizontally. As attack types have different number of associated captures (see Table 1), we compute the average in each attack category and report a single heatmap summarizing the performance in a specific category. As the standard deviation from this aggregation is negligible with respect to the average, we do not present associated figures here. The results are rounded at two decimal places. Specifically, we vary the window length (i.e., ω from 50 to 400 samples in increments of 50 samples) and the offset (i.e., δ from 10 to ω in increments of 10 samples).

Fig. 4 shows results for the Matrix Correlation Distribution Method. We found that overall, this method tends to perform better at detecting the `light_off_attack` as many of the heatmap cells are above AUC-ROC of 0.70 (see greater proportion of redder cells placed in the heatmap). Moreover, we observe that there is a region of better performance for the `max_engine_attack` characterized for lower values of $\omega \leq 300$ and $\delta \leq 100$. Interestingly, among the highest performances across attack types is the `correlated_attack` with an AUC-ROC of 0.77 for the combination ($\omega = 300, \delta = 270$). We also observed that for the `max_speedometer_attack` and `light_on_attack`

the reported AUC-ROC tends to be below 0.50 in most of the combinations of ω and δ . This suggests that the Matrix Correlation Distribution Method has a hard time detecting these attacks as the probability of ranking random positive windows more highly than random negatives windows is below 0.50 in most of the ω and δ combinations.

Fig. 5 shows results for the Matrix Correlation Correlation Method. We observe that the highest detection performance is obtained for the `correlated_attack` with an AUC-ROC of 0.89 for the combination ($\omega = 150, \delta = 130$). We also observe AUC-ROC values above 0.70 for the `correlated_attack` that tend to be generally contained at lower values of ω and δ , i.e., $\omega \leq 200$ and $\delta \leq 150$. Note that the evaluation metrics for the remaining attacks (i.e., `max_speedometer_attack`, `max_engine_attack`, and `light_on_attack`) are not as good as in the previous attacks barely staying above 0.50. An exception is the `light_off_attack` where AUC-ROC values around 0.70 are contained at lower values of ω and δ , i.e., $\omega \leq 150$ and $\delta \leq 150$.

Fig. 6 shows results for the Ganesan17 Method. We observe that the highest evaluation metric is achieved for the `max_speedometer_attack` at 0.74 for the combination ($\omega = 400, \delta = 380$). For this attack, we also found a region where AUC-ROC rose 0.70 specially contained at lower values of ω and δ , i.e., $100 \leq \omega \leq 150$ and $\delta \leq 160$. For the remaining attack types we did not find any other remarkable evaluation metrics.

Fig. 7 shows results for the Moriano22 Method. We observe that the maximum AUC-ROC among attack types is achieved with the `max_engine_attack` achieving an AUC-ROC of 1.00 for a few combinations of ω and δ . Additionally, for this attack, we found a region where AUC-ROC rose 0.70 that is contained at lower values of ω and δ , i.e., $100 \leq \omega \leq 400$ and $10 \leq \delta \leq 160$. For the `light_off_attack`, we also observe a performance region with values of AUC-ROC above 0.70, generally contained at lower values of ω and δ , i.e., $\omega \leq 200$ and $\delta \leq 200$. This method also displays AUC-ROC values above 0.60 for the `light_on_attack` generally contained at the entire domain of values of ω and δ . In addition, we observe that the evaluation metrics for the remaining attacks (i.e., `correlated_attack` and `max_speedometer_attack`) are not as good as in the previous attacks barely reaching above 0.50.

5.2 Evaluation Metrics Summary

Table 2 summarizes results extracted from the heatmaps. We place attack categories in the rows and attack detection methods in the columns. This means that each cell in this table shows the performance of a specific detection method in a particular attack from the ROAD dataset. We focus on summary statistics including the mean (μ), standard deviation (σ), median (η), minimum (min) and maximum (max). We also show the average and standard deviations from the maximum values for each attack detection methods and attack types in the ROAD dataset. They are displayed in the last row and column in the table.

Notably, from the attack detection methods, Moriano22 Method performs the best across attacks (i.e., $\overline{max} = 0.73$),

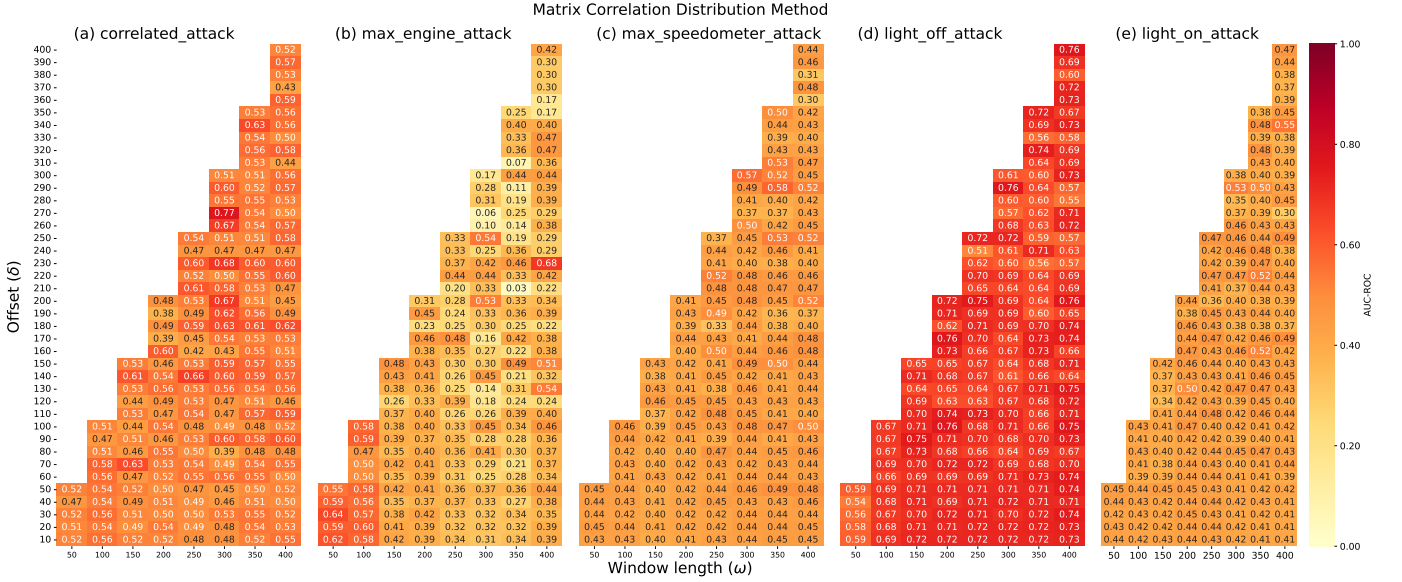


Fig. 4. AUC-ROC over different window length and offset combinations for the *Matrix Correlation Distribution* method on the different attacks in the ROAD dataset: (a) correlated attack, (b) max engine coolant temperature attack, (c) max speedometer attack, (d) reverse light off attack, and (e) reverse light on attack.

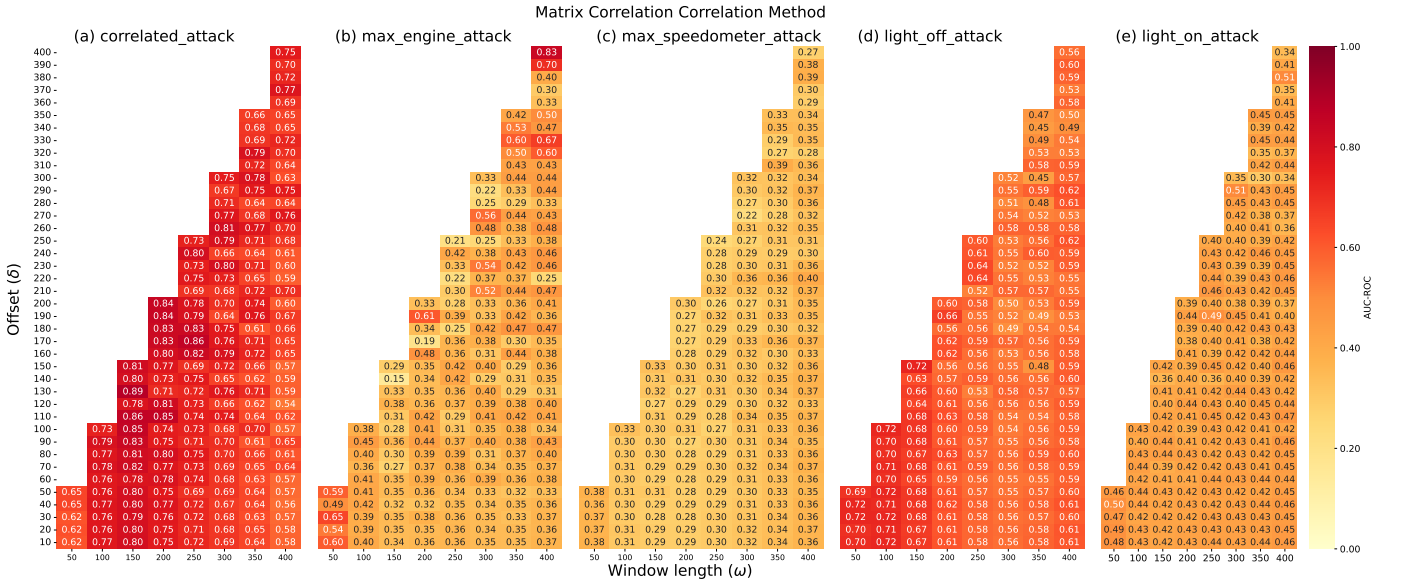


Fig. 5. AUC-ROC over different window length and offset combinations for the *Matrix Correlation Correlation* method on the different attacks in the ROAD dataset: (a) correlated attack, (b) max engine coolant temperature attack, (c) max speedometer attack, (d) reverse light off attack, and (e) reverse light on attack.

followed by Matrix Correlation Distribution and Matrix Correlation Correlation (i.e., $\overline{max} = 0.67$), and Ganesan17 (i.e., $\overline{max} = 0.61$). Among these, the minimum and maximum variation of maximum AUC-ROC is obtained by *light_on_attack* (i.e., $\sigma_{max} = 0.00$) and *max_engine_attack* (i.e., $\sigma_{max} = 0.17$) respectively.

Note that, from the attack categories, the *max_engine_attack* was found to be the attack that is detected with higher AUC-ROC among benchmarked algorithms (i.e., $\overline{max} = 0.79$), followed by *correlated_attack* (i.e., $\overline{max} = 0.73$), *light_off_attack* (i.e., $\overline{max} = 0.67$) and *max_speedometer_attack* and *light_on_attack*

(i.e., $\overline{max} = 0.59$). Among these, the minimum and maximum variation of maximum AUC-ROC is obtained by *light_on_attack* (i.e., $\sigma_{max} = 0.00$) and *max_engine_attack* (i.e., $\sigma_{max} = 0.17$) respectively.

Finally, Fig. 8 compares each detection method on the basis of summary statistics for each of attack type using dot plots. A desirable online algorithm for detecting masquerade attacks in CAN by processing streams of time series data should have high values of μ , η , min, and max and lower values of σ in the range $[0, 1]$. We notice that there is no free lunch in the detection of masquerade attacks in CAN in an online setting as there is no single algorithm that is optimal for detecting each attack type. Notably, Ganesan17,

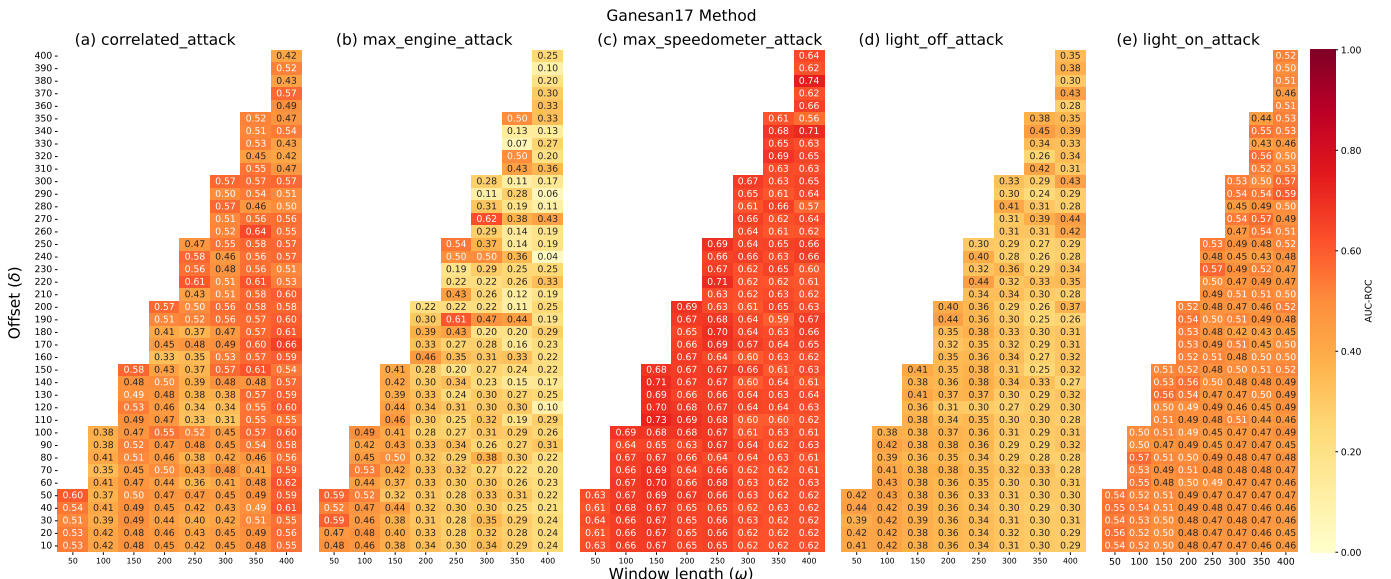


Fig. 6. AUC-ROC over different window length and offset combinations for the *Ganesan17* method on the different attacks in the ROAD dataset: (a) correlated attack, (b) max engine coolant temperature attack, (c) max speedometer attack, (d) reverse light off attack, and (e) reverse light on attack.

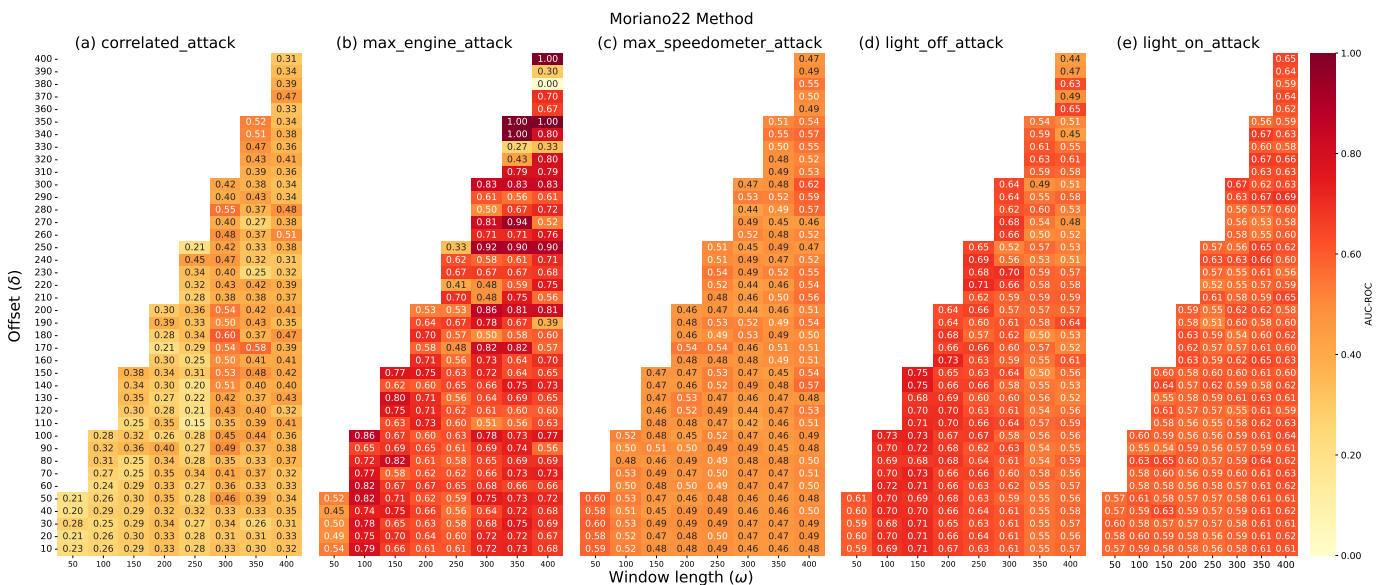


Fig. 7. AUC-ROC over different window length and offset combinations for the *Moriano22* method on the different attacks in the ROAD dataset: (a) correlated attack, (b) max engine coolant temperature attack, (c) max speedometer attack, (d) reverse light off attack, and (e) reverse light on attack.

the worst performing algorithms across all attack types is the best performing detection algorithm for the hardest attack to detect, i.e., *max_speedometer_attack*.

5.3 Performance Metrics Summary

Table 3 summarizes TTW results based on heatmaps that we do not display here. We place attack categories in the rows and attack detection methods in the columns. This means that each cell in this table shows the TTW of a specific detection method in a particular attack from the ROAD dataset. We focus on summary statistics including the mean (μ), standard deviation (σ), median (η), minimum (min), and maximum (max). In addition, we also show the average

and standard deviations from the minimum values for each attack detection methods and attack types in the ROAD dataset. They are displayed as the last row and column in the table.

Notably, from the attack detection methods, Matrix Correlation Distribution is the quickest across attacks (i.e., $\overline{\min} = 0.33$), followed by Matrix Correlation Correlation (i.e., $\overline{\min} = 2.53$), Ganesan17 (i.e., $\overline{\min} = 3.65$), and Moriano22 (i.e., $\overline{\min} = 8.42$). Among these, the minimum and maximum variation of maximum TTW is obtained by Matrix Correlation Distribution (i.e., $\sigma_{\min} = 0.00$) and Moriano22 (i.e., $\sigma_{\min} = 0.51$) respectively.

In addition, from the attack categories, we found

TABLE 2

Summary of evaluation metrics based on the AUC-ROC heatmaps. We show the mean (μ), standard deviation (σ), median (η), minimum (min) including the combination of window length and offset that produces it, and maximum (max) including the combination of window length and offset that produces it. Attack types are placed in the rows while detection methods are placed in the columns. We also report averages and standard deviation of the maximum values obtained by each attack and detection method denoted by \overline{max} and σ_{max} .

Attack/Method	Matrix Correlation Distribution	Matrix Correlation Correlation	Ganesan17	Moriano22	
correlated_attack	$\mu = 0.53$ $\sigma = 0.06$ $\eta = 0.53$ min = 0.38 (200, 190) max = 0.77 (300, 270)	$\mu = 0.71$ $\sigma = 0.07$ $\eta = 0.72$ min = 0.54 (400, 120) max = 0.88 (150, 130)	$\mu = 0.49$ $\sigma = 0.07$ $\eta = 0.49$ min = 0.31 (300, 110) max = 0.66 (400, 170)	$\mu = 0.35$ $\sigma = 0.08$ $\eta = 0.34$ min = 0.15 (250, 110) max = 0.60 (300, 180)	$\overline{max} = 0.73$ $\sigma_{max} = 0.12$
max_engine_attack	$\mu = 0.36$ $\sigma = 0.11$ $\eta = 0.36$ min = 0.03 (350, 210) max = 0.68 (400, 230)	$\mu = 0.38$ $\sigma = 0.09$ $\eta = 0.37$ min = 0.15 (150, 140) max = 0.83 (400, 400)	$\mu = 0.31$ $\sigma = 0.11$ $\eta = 0.29$ min = 0.04 (400, 240) max = 0.63 (300, 270)	$\mu = 0.66$ $\sigma = 0.13$ $\eta = 0.67$ min = 0.00 (400, 380) max = 1.00 (400, 400)	$\overline{max} = 0.79$ $\sigma_{max} = 0.17$
max_speedometer_attack	$\mu = 0.44$ $\sigma = 0.04$ $\eta = 0.43$ min = 0.30 (400, 360) max = 0.58 (350, 290)	$\mu = 0.32$ $\sigma = 0.03$ $\eta = 0.31$ min = 0.22 (300, 270) max = 0.40 (400, 220)	$\mu = 0.64$ $\sigma = 0.03$ $\eta = 0.64$ min = 0.56 (400, 350) max = 0.74 (400, 380)	$\mu = 0.49$ $\sigma = 0.03$ $\eta = 0.49$ min = 0.42 (300, 100) max = 0.62 (400, 300)	$\overline{max} = 0.59$ $\sigma_{max} = 0.14$
light_off_attack	$\mu = 0.68$ $\sigma = 0.05$ $\eta = 0.69$ min = 0.51 (250, 240) max = 0.76 (400, 400)	$\mu = 0.59$ $\sigma = 0.06$ $\eta = 0.58$ min = 0.45 (350, 300) max = 0.72 (150, 150)	$\mu = 0.34$ $\sigma = 0.05$ $\eta = 0.34$ min = 0.24 (350, 290) max = 0.45 (350, 340)	$\mu = 0.61$ $\sigma = 0.06$ $\eta = 0.61$ min = 0.44 (400, 400) max = 0.75 (150, 140)	$\overline{max} = 0.67$ $\sigma_{max} = 0.15$
light_on_attack	$\mu = 0.42$ $\sigma = 0.03$ $\eta = 0.43$ min = 0.29 (400, 270) max = 0.55 (400, 340)	$\mu = 0.42$ $\sigma = 0.03$ $\eta = 0.42$ min = 0.28 (350, 300) max = 0.51 (300, 290)	$\mu = 0.49$ $\sigma = 0.03$ $\eta = 0.49$ min = 0.42 (300, 180) max = 0.59 (400, 290)	$\mu = 0.59$ $\sigma = 0.03$ $\eta = 0.59$ min = 0.51 (250, 190) max = 0.69 (400, 290)	$\overline{max} = 0.59$ $\sigma_{max} = 0.08$
	$\overline{max} = 0.67$ $\sigma_{max} = 0.10$	$\overline{max} = 0.67$ $\sigma_{max} = 0.21$	$\overline{max} = 0.61$ $\sigma_{max} = 0.11$	$\overline{max} = 0.73$ $\sigma_{max} = 0.16$	

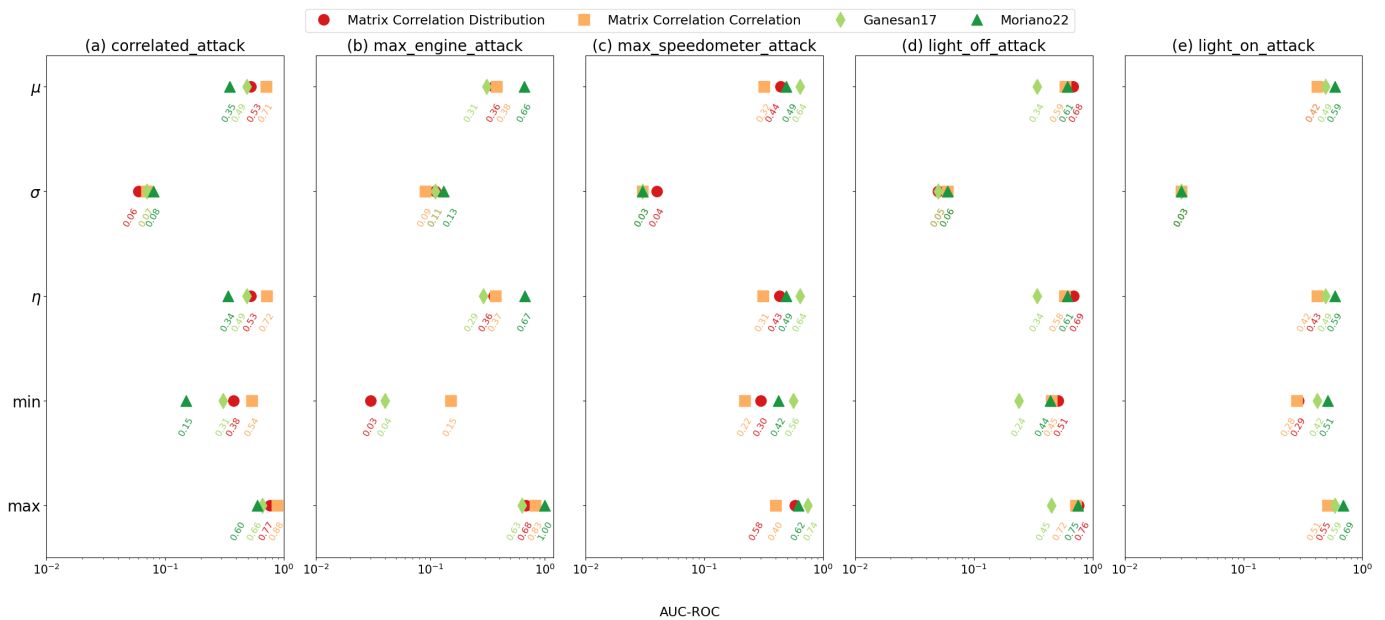


Fig. 8. Dot plots comparing each detection method based on summary statistics of AUC-ROC per attack type: (a) correlated_attack, (b) max_engine_attack, (c) max_speedometer_attack, (d) light_off_attack, and (e) light_on_attack.

that there are no outstanding variations on the light_off_attack) to 3.89 (light_on_attack) on TTW within attack categories varying from 3.58 (i.e., average).

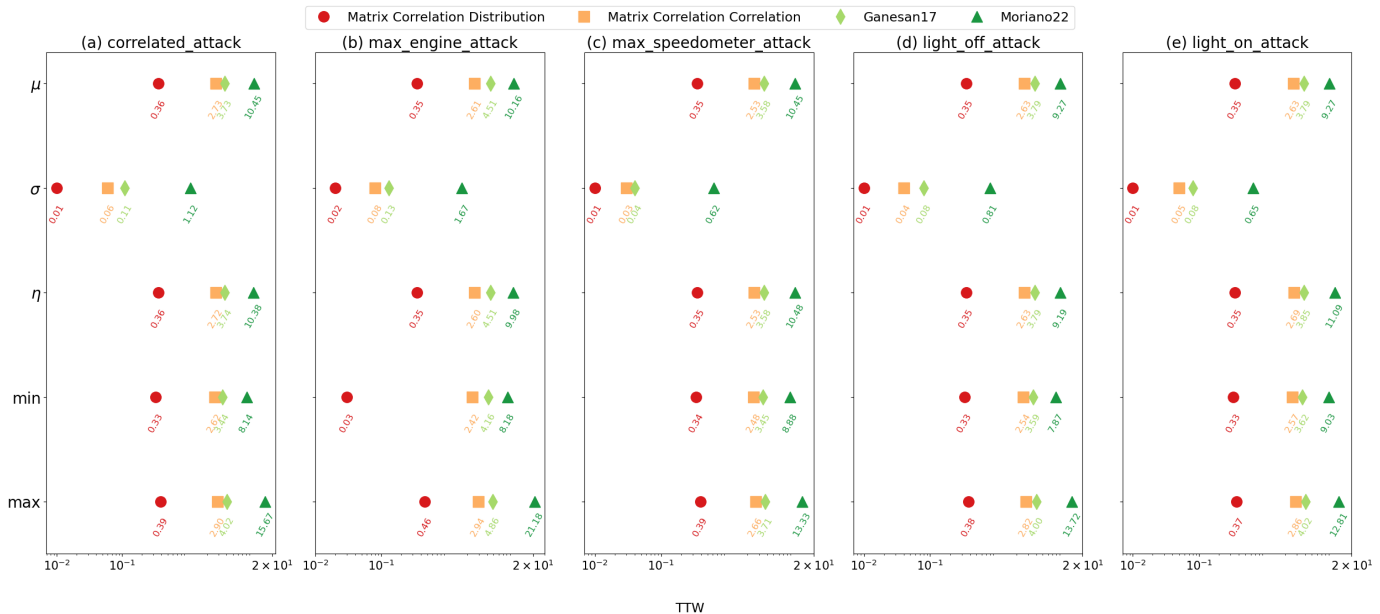


Fig. 9. Dot plots comparing each detection method based on summary statistics of TTW per attack type: (a) `correlated_attack`, (b) `max_engine_attack`, (c) `max_speedometer_attack`, (d) `light_off_attack`, and (e) `light_on_attack`.

Finally, Fig. 9 compares each detection method on the basis of TTW summary statistics for each attack type using dot plots. A desirable online algorithm for detecting masquerade attacks in CAN by processing streams of time series data should have low values of μ , η , min, max and lower values of σ in the range $[0, 1]$. Remarkably, Matrix Correlation Distribution method is the quickest detection algorithm one order of magnitude lower than the others.

6 DISCUSSION

In this work, we have benchmarked non-DL-based unsupervised online IDS for detecting masquerade attacks in CAN data. Our results indicate that the benchmarked algorithms are not equally effective at detecting every attack type as it has been shown before in previous studies in the offline setting [18], [33], [34]. We attributed this to the foundational principle used for each of the detection algorithms and the magnitude of the perturbation that is incurred when introducing each of the attacks. Overall, Moriano22 produces the best detection results across attack types. Among attacks, `max_speedometer_attack` and `light_on_attack` are the overall hardest to detect attack type.

In agreement with the foundational principle of Moriano22 (i.e., finding disruptions in the hierarchy of time series clusters), our results supports the fact that introduced masquerade attacks in the ROAD dataset change the relative hierarchy of time series clusters as it was shown previously in an offline setting in [15]. As opposed to Ganesan17, which focuses on significant deviations of time series cluster assignments, Moriano22 captures significant deviations in the hierarchy of clusters. Contrary to our intuition, our findings also reveal that Matrix Correlation Distribution and Matrix Correlation Correlation methods perform better than Ganesan17. We suspect that this is in part because of the multiple hyperparameters that need to be adjusted in Ganesan17 to tune its optimal performance.

While previous research has focused on detecting masquerade attacks in an offline setting, our results demonstrate the importance of considering how sliding windows are processed in an online setting with respect to window length and offset. Specifically, our results provide new insights on the effect of choosing carefully these two data partitioning parameters. To make benchmarked methods more effective to work in a real-world setting, online algorithms should strive to perform well when processing small batches of data (i.e., lower ω values) and low latency between window transitions (i.e., lower δ values). We quantify these relationships for every method on each of the attack types.

Our study provides insights on the effectiveness and performance of online detection algorithms for detecting masquerade attacks from the ROAD dataset. Having noted the strengths of our benchmark framework, we are also aware of the following limitations of our proposed work.

Lack of Validation in a Real Environment: Our proposed framework partitions logs of already collected CAN captures to simulate an streaming environment of CAN data using windows. We did not empirically validated our results on a moving vehicle including the necessary hardware and performance tuning involved to do so.

Limited Number of Benchmarked Algorithms: We benchmarked four unsupervised online detection algorithms. As we strive for computationally efficient approaches and test their efficacy on a widely known attack dataset, we did not include unsupervised DL-based approaches (e.g., [16], [19]) in the comparison.

Focus on a Single Testbed Dataset: We used the ROAD dataset with a limited number of masquerade attacks to benchmark online detection algorithms. We did not consider newer datasets with a higher number of masquerade attacks generated on modern automobiles [59].

Use of Default Parameter Values in Detection Algorithms: We used default parameters values as the original algo-

TABLE 3

Summary of evaluation metrics based on TTW in milliseconds. We show the mean (μ), standard deviation (σ), median (η), minimum (min) including the combination of window length and offset that produces it, and maximum (max) including the combination of window length and offset that produces it. Attack types are placed in the rows while detection methods are placed in the columns. We also report averages and standard deviation of the minimum values obtained by each attack and detection method denoted by \overline{min} and σ_{min} .

Attack/Method	Matrix Correlation Distribution	Matrix Correlation Correlation	Ganesan17	Moriano22	
correlated_attack	$\mu = 0.36$ $\sigma = 0.01$ $\eta = 0.36$ min = 0.33 (50, 40) max = 0.39 (400, 320)	$\mu = 2.73$ $\sigma = 0.06$ $\eta = 2.72$ min = 2.62 (100, 30) max = 2.90 (250, 140)	$\mu = 3.73$ $\sigma = 0.11$ $\eta = 3.74$ min = 3.44 (250, 240) max = 4.02 (350, 250)	$\mu = 10.45$ $\sigma = 1.12$ $\eta = 10.38$ min = 8.14 (50, 20) max = 15.67 (300, 160)	$\overline{min} = 3.63$ $\sigma_{min} = 3.28$
max_engine_attack	$\mu = 0.35$ $\sigma = 0.02$ $\eta = 0.35$ min = 0.03 (150, 10) max = 0.46 (150, 140)	$\mu = 2.61$ $\sigma = 0.08$ $\eta = 2.60$ min = 2.42 (100, 60) max = 2.94 (400, 360)	$\mu = 4.51$ $\sigma = 0.13$ $\eta = 4.51$ min = 4.16 (50, 50) max = 4.86 (400, 270)	$\mu = 10.16$ $\sigma = 1.67$ $\eta = 9.98$ min = 8.18 (50, 40) max = 21.18 (350, 3300)	$\overline{min} = 3.77$ $\sigma_{min} = 3.33$
max_speedometer_attack	$\mu = 0.35$ $\sigma = 0.01$ $\eta = 0.35$ min = 0.34 (50, 20) max = 0.39 (100, 90)	$\mu = 2.53$ $\sigma = 0.03$ $\eta = 2.53$ min = 2.48 (250, 240) max = 2.66 (100, 80)	$\mu = 3.58$ $\sigma = 0.04$ $\eta = 3.58$ min = 3.45 (300, 270) max = 3.71 (100, 80)	$\mu = 10.45$ $\sigma = 0.62$ $\eta = 10.48$ min = 8.88 (50, 40) max = 13.33 (400, 340)	$\overline{min} = 3.79$ $\sigma_{min} = 3.64$
light_off_attack	$\mu = 0.35$ $\sigma = 0.01$ $\eta = 0.35$ min = 0.33 (50, 30) max = 0.38 (300, 220)	$\mu = 2.63$ $\sigma = 0.04$ $\eta = 2.63$ min = 2.54 (100, 60) max = 2.82 (400, 350)	$\mu = 3.79$ $\sigma = 0.08$ $\eta = 3.79$ min = 3.59 (350, 340) max = 4.00 (400, 200)	$\mu = 9.27$ $\sigma = 0.81$ $\eta = 9.19$ min = 7.87 (50, 60) max = 13.72 (400, 260)	$\overline{min} = 3.58$ $\sigma_{min} = 3.16$
light_on_attack	$\mu = 0.35$ $\sigma = 0.01$ $\eta = 0.35$ min = 0.33 (50, 40) max = 0.37 (400, 180)	$\mu = 2.63$ $\sigma = 0.05$ $\eta = 2.69$ min = 2.57 (400, 380) max = 2.86 (200, 200)	$\mu = 3.79$ $\sigma = 0.08$ $\eta = 3.85$ min = 3.62 (100, 90) max = 4.02 (350, 290)	$\mu = 9.27$ $\sigma = 0.65$ $\eta = 11.09$ min = 9.03 (50, 40) max = 12.81 (400, 320)	$\overline{min} = 3.89$ $\sigma_{min} = 3.69$
	$\overline{min} = 0.33$ $\sigma_{min} = 0.00$	$\overline{min} = 2.53$ $\sigma_{min} = 0.08$	$\overline{min} = 3.65$ $\sigma_{min} = 0.30$	$\overline{min} = 8.42$ $\sigma_{min} = 0.51$	

rithms in Ganesan17 and Moriano22. Therefore we did not explore the use of hyperparameter tuning on these algorithms that could have an effect in their performance.

We anticipate that field experiments on a moving vehicle can be performed to validate our results based on new technologies being deployed to extract time series data from CAN payloads (e.g., [46]).

7 CONCLUSION

This paper benchmarks non-DL-based unsupervised online IDS for detecting masquerade attacks in CAN. We focus on four detection algorithms (i.e., Matrix Correlation Distribution, Matrix Correlation Correlation, Ganesan17 [23], and Moriano22 [15]) which foundational mechanism is based on capturing significant deviations from expected pairwise correlations over a stream of multivariate time series. The inclusion of these baseline algorithms along with their open source implementation allow direct comparison with forthcoming online algorithms in this research space. The presented benchmark differs from other benchmarks in prior works in that it focuses on the online operation of detection algorithms (as opposed to offline operation mode) aimed at detecting masquerade attacks—the stealthiest category of attacks in the CAN bus. Our benchmark is based on the concept of time windows that control the partition of a stream of time series. Specifically, we use sliding windows,

with respect to the number of observations, to analyze variations in the AUC-ROC based on different combinations of window length and offset. We report conditions that makes benchmarked algorithms more successful than others for certain attack types as well as a summary of their overall performance on different attacks. We show that overall, Moriano22 performs the best at detecting the different attack types in the ROAD dataset. Our analysis reveals that the max_speedometer_attack is the more elusive to detect among detection algorithms.

Future work in this area involve the inclusion of more recent online detection algorithms such as the work by Shahriar et al. [17] and the validation of our results in an empirical moving vehicle setting.

ACKNOWLEDGEMENTS

This manuscript has been authored by UT-Battelle, LLC under Contract No. DE-AC05-00OR22725 with the U.S. Department of Energy. The publisher, by accepting the article for publication, acknowledges that the U.S. Government retains a non-exclusive, paid up, irrevocable, world-wide license to publish or reproduce the published form of the manuscript, or allow others to do so, for U.S. Government purposes. The DOE will provide public access to these results in accordance with the DOE Public Access Plan (<http://energy.gov/downloads/doe-public-access-plan>).

This research was sponsored in part by Oak Ridge National Laboratory's (ORNL's) Laboratory Directed Research and Development program and by the DOE. There was no additional external funding received for this study. This research used birthright cloud resources of the Compute and Data Environment for Science (CADES) at the Oak Ridge National Laboratory, which is supported by the Office of Science of the U.S. Department of Energy under Contract No. DE-AC05-00OR22725. The funders had no role in study design, data collection and analysis, decision to publish, or preparation of this manuscript.

REFERENCES

- [1] M. T. Kawser, M. S. Fahad, S. Ahmed, S. S. Sajjad, and H. A. Rafi, "The perspective of vehicle-to-everything (v2x) communication towards 5g," *IJCSNS*, vol. 19, no. 4, p. 146, 2019.
- [2] O. Minawi, J. Whelan, A. Almechadi, and K. El-Khatib, "Machine learning-based intrusion detection system for controller area networks," in *Proceedings of the 10th ACM Symposium on Design and Analysis of Intelligent Vehicular Networks and Applications*, 2020, pp. 41–47.
- [3] A. Buscemi, I. Turcanu, G. Castignani, A. Panchenko, T. Engel, and K. G. Shin, "A survey on controller area network reverse engineering," *IEEE Commun. Sur. Tut.*, 2023.
- [4] I. Standard, "Road vehicles—controller area network (can) - part 2: Low-speed fault-tolerant," *ISO*, vol. 11898-3, p. 1, 2006.
- [5] —, "Road vehicles—controller area network (can)—part 1: Data link layer and physical signalling," *ISO*, vol. 11898-1, p. 1, 2015.
- [6] —, "Road vehicles—controller area network (can) - part 2: High-speed medium access unit," *ISO*, vol. 11898-2, p. 1, 2016.
- [7] C. Miller and C. Valasek, "Remote exploitation of an unaltered passenger vehicle," *Black Hat USA*, vol. 2015, p. 91, 2015.
- [8] —, "CAN message injection: OG dynamite edition," *Tech. Rep.*, 2016.
- [9] K.-T. Cho and K. G. Shin, "Fingerprinting electronic control units for vehicle intrusion detection," in *Proceedings of the 25th USENIX Security Symposium*, 2016, pp. 911–927.
- [10] M. E. Verma, R. A. Bridges, M. D. Iannacone, S. C. Hollifield, P. Moriano, S. C. Hespeler, B. Kay, and F. L. Combs, "A comprehensive guide to can ids data and introduction of the road dataset," *PLOS ONE*, vol. 19, no. 1, pp. 1–32, 01 2024. [Online]. Available: <https://doi.org/10.1371/journal.pone.0296879>
- [11] S. Woo, H. J. Jo, and D. H. Lee, "A practical wireless attack on the connected car and security protocol for in-vehicle can," *IEEE Transactions on Intell. Transp.*, vol. 16, no. 2, pp. 993–1006, 2014.
- [12] H. J. Jo and W. Choi, "A survey of attacks on controller area networks and corresponding countermeasures," *IEEE Transactions on Intell. Transp.*, vol. 23, no. 7, pp. 6123–6141, 2021.
- [13] F. Akowuah and F. Kong, "Physical invariant based attack detection for autonomous vehicles: Survey, vision, and challenges," in *2021 Fourth International conference on connected and autonomous driving (MetroCAD)*. IEEE, 2021, pp. 31–40.
- [14] M. R. Ansari, W. T. Miller, C. She, and Q. Yu, "A low-cost masquerade and replay attack detection method for can in automobiles," in *2017 IEEE international symposium on circuits and systems (ISCAS)*. IEEE, 2017, pp. 1–4.
- [15] P. Moriano, R. A. Bridges, and M. D. Iannacone, "Detecting can masquerade attacks with signal clustering similarity," in *Proceedings Fourth International Workshop on Automotive and Autonomous Vehicle Security*, ser. AutoSec 2022. Internet Society, 2022. [Online]. Available: <http://dx.doi.org/10.14722/autosec.2022.23028>
- [16] M. H. Shahriar, Y. Xiao, P. Moriano, W. Lou, and Y. T. Hou, "Canshield: Deep-learning-based intrusion detection framework for controller area networks at the signal level," *IEEE Internet Things*, vol. 10, no. 24, pp. 22 111–22 127, 2023.
- [17] M. H. Shahriar, W. Lou, and Y. T. Hou, "CANtropy: Time series feature extraction-based intrusion detection systems for controller area networks," in *Symposium on Vehicles Security and Privacy*. Internet Society, 2023. [Online]. Available: <https://dx.doi.org/10.14722/vehiclesec.2023.23090>
- [18] S. Sharmin, H. Mansor, A. F. Abdul Kadir, and N. A. Aziz, "Comparative Evaluation of Anomaly-Based Controller Area Network IDS," in *Proceedings of the 12th International Conference on Software and Computer Applications*, 2023, pp. 218–226.
- [19] M. Hanselmann, T. Strauss, K. Dormann, and H. Ulmer, "Canet: An unsupervised intrusion detection system for high dimensional can bus data," *IEEE Access*, vol. 8, pp. 58 194–58 205, 2020.
- [20] A. Nichelini, C. A. Pozzoli, S. Longari, M. Carminati, and S. Zanero, "Canova: a hybrid intrusion detection framework based on automatic signal classification for can," *Comput. Secur.*, vol. 128, p. 103166, 2023.
- [21] H. Ji, Y. Wang, H. Qin, Y. Wang, and H. Li, "Comparative performance evaluation of intrusion detection methods for in-vehicle networks," *IEEE Access*, vol. 6, pp. 37 523–37 532, 2018.
- [22] S. Sharmin, H. Mansor, A. F. A. Kadir, and N. A. Aziz, "Benchmarking frameworks and comparative studies of controller area network (can) intrusion detection systems: A review," *arXiv preprint arXiv:2402.06904*, 2024.
- [23] A. Ganesan, J. Rao, and K. Shin, "Exploiting consistency among heterogeneous sensors for vehicle anomaly detection," SAE Technical Paper, Tech. Rep., 2017.
- [24] B. Babcock, M. Datar, and R. Motwani, "Sampling from a moving window over streaming data," in *Proceedings of the thirteenth annual ACM-SIAM symposium on Discrete algorithms*, 2002, pp. 633–634.
- [25] J. Gama, "A survey on learning from data streams: current and future trends," *Lect. Notes. Artif. Int.*, vol. 1, pp. 45–55, 2012.
- [26] P. Moriano, "Code: Benchmarking online ids for masquerade attacks in can," <https://github.com/pmoriano/benchmarking-unsupervised-online-IDS-masquerade-attacks>, 2024.
- [27] K.-T. Cho and K. G. Shin, "Error Handling of In-vehicle Networks Makes Them Vulnerable," in *Proceedings of the 2016 ACM SIGSAC Conference on Computer and Communications Security*, 2016, p. 1044–1055.
- [28] C. Miller and C. Valasek, "Can message injection," *OG Dynamite Edition*, 2016.
- [29] G. Dupont, J. Den Hartog, S. Etalle, and A. Lekidis, "Evaluation framework for network intrusion detection systems for in-vehicle can," in *2019 IEEE International Conference on Connected Vehicles and Expo (ICCVE)*. IEEE, 2019, pp. 1–6.
- [30] H. Lee, S. H. Jeong, and H. K. Kim, "Otidis: A novel intrusion detection system for in-vehicle network by using remote frame," in *2017 15th Annual Conference on Privacy, Security and Trust (PST)*. IEEE, 2017, pp. 57–5709.
- [31] S. Stachowski, R. Gaynier, and D. J. LeBlanc, "An assessment method for automotive intrusion detection system performance," University of Michigan, Ann Arbor, Transportation Research Institute, Tech. Rep., 2019.
- [32] D. H. Blevins, P. Moriano, R. A. Bridges, M. E. Verma, M. D. Iannacone, and S. C. Hollifield, "Time-based can intrusion detection benchmark," in *Proceedings Fourth International Workshop on Automotive and Autonomous Vehicle Security*, ser. AutoSec 2021. Internet Society, 2021. [Online]. Available: <https://doi.org/10.14722/autosec.2021.23013>
- [33] P. Agbaje, A. Anjum, A. Mitra, G. Bloom, and H. Olufowobi, "A framework for consistent and repeatable controller area network ids evaluation," in *Proceedings of the Fourth International Workshop on Automotive and Autonomous Vehicle Security*, 2022. [Online]. Available: <http://dx.doi.org/10.14722/autosec.2022.23031>
- [34] F. Pollicino, D. Stabili, and M. Marchetti, "Performance comparison of timing-based anomaly detectors for controller area network: a reproducible study," *ACM Transactions on Cyber-Physical Systems*, 2023.
- [35] D. Chicco and G. Jurman, "The advantages of the matthews correlation coefficient (mcc) over f1 score and accuracy in binary classification evaluation," *BMC Genomics*, vol. 21, pp. 1–13, 2020.
- [36] A. K. Desta, S. Ohira, I. Arai, and K. Fujikawa, "Id sequence analysis for intrusion detection in the can bus using long short term memory networks," in *2020 IEEE International Conference on Pervasive Computing and Communications Workshops (PerCom Workshops)*, 2020, pp. 1–6.
- [37] J. Sunny, S. Sankaran, and V. Saraswat, "A hybrid approach for fast anomaly detection in controller area networks," in *2020 IEEE International Conference on Advanced Networks and Telecommunications Systems (ANTS)*. IEEE, 2020, pp. 1–6.
- [38] M. Jedh, J. K. Lee *et al.*, "Evaluation of the architecture alternatives for real-time intrusion detection systems for vehicles," in 2022

IEEE 22nd International Conference on Software Quality, Reliability and Security (QRS). IEEE, 2022, pp. 864–873.

- [39] H. Jadidbonab, A. Tomlinson, H. N. Nguyen, T. Doan, and S. Shaikh, "A realtime in-vehicle network testbed for machine learning-based ids training and validation," in *Workshop on AI and Cybersecurity: co-located with 41st SGAI International Conference on Artificial Intelligence (SGAI 2021)*. CEUR Workshop Proceedings, 2022.
- [40] J. Gama, I. Žliobaitė, A. Bifet, M. Pechenizkiy, and A. Bouchachia, "A survey on concept drift adaptation," *ACM Comput. Surv.*, vol. 46, no. 4, pp. 1–37, 2014.
- [41] P. Avogadro, L. Palonca, and M. A. Dominoni, "Online anomaly search in time series: significant online discords," *Knowl. Inf. Syst.*, vol. 62, no. 8, pp. 3083–3106, 2020.
- [42] E. M. Ferragut, J. Laska, and R. A. Bridges, "A new, principled approach to anomaly detection," in *2012 11th International Conference on Machine Learning and Applications*, vol. 2. IEEE, 2012, pp. 210–215.
- [43] S. Checkoway, D. McCoy, B. Kantor, D. Anderson, H. Shacham, S. Savage, K. Koscher, A. Czeskis, F. Roesner, and T. Kohno, "Comprehensive experimental analyses of automotive attack surfaces," in *20th USENIX security symposium (USENIX Security 11)*, 2011.
- [44] T. Qin, Z. Liu, P. Wang, S. Li, X. Guan, and L. Gao, "Symmetry degree measurement and its applications to anomaly detection," *IEEE T. Inf. Foren. Sec.*, vol. 15, pp. 1040–1055, 2019.
- [45] M. D. Pesé, T. Stacer, C. A. Campos, E. Newberry, D. Chen, and K. G. Shin, "Librecan: Automated can message translator," in *Proceedings of the 2019 ACM SIGSAC Conference on Computer and Communications Security*, 2019, pp. 2283–2300.
- [46] M. E. Verma, R. A. Bridges, J. J. Sosnowski, S. C. Hollifield, and M. D. Iannacone, "Can-d: A modular four-step pipeline for comprehensively decoding controller area network data," *IEEE T. Veh. Technol.*, vol. 70, no. 10, pp. 9685–9700, 2021.
- [47] A. Buscemi, I. Turcanu, G. Castignani, R. Crunelle, and T. Engel, "Canmatch: a fully automated tool for can bus reverse engineering based on frame matching," *IEEE T. Veh. Technol.*, vol. 70, no. 12, pp. 12 358–12 373, 2021.
- [48] K. Pearson, "Notes on regression and inheritance in the case of two parents," *P. R. Soc. London*, vol. 58, pp. 240–242, 1895.
- [49] H. B. Mann and D. R. Whitney, "On a test of whether one of two random variables is stochastically larger than the other," *The Annals of Mathematical Statistics*, pp. 50–60, 1947.
- [50] C. Spearman, "The proof and measurement of association between two things," *The American Journal of Psychology*, pp. 441–471, 1987.
- [51] P. Schober, C. Boer, and L. A. Schwarte, "Correlation coefficients: appropriate use and interpretation," *Anesth. Analg.*, vol. 126, no. 5, pp. 1763–1768, 2018.
- [52] M. Ester, H.-P. Kriegel, J. Sander, and X. Xu, "A density-based algorithm for discovering clusters in large spatial databases with noise," in *Proceedings of the Second International Conference on Knowledge Discovery and Data Mining (KDD)*, 1996, p. 226–231.
- [53] StackExchange CrossValidated, "Converting similarity matrix to (euclidean) distance matrix," <https://stats.stackexchange.com/questions/36152/converting-similarity-matrix-to-euclidean-distance-matrix/36158#36158>, online; cessed: 2024-02-28.
- [54] A. K. Jain, M. N. Murty, and P. J. Flynn, "Data clustering: a review," *ACM Comput. Surv.*, vol. 31, no. 3, pp. 264–323, 1999.
- [55] A. J. Gates and Y.-Y. Ahn, "Clusim: a python package for calculating clustering similarity," *Journal of Open Source Software*, vol. 4, no. 35, p. 1264, 2019.
- [56] A. J. Gates, I. B. Wood, W. P. Hetrick, and Y.-Y. Ahn, "Element-centric clustering comparison unifies overlaps and hierarchy," *Sci. Rep.*, vol. 9, no. 1, p. 8574, 2019.
- [57] T. Fawcett, "An introduction to roc analysis," *Pattern Recogn. lett.*, vol. 27, no. 8, pp. 861–874, 2006.
- [58] J. Davis and M. Goadrich, "The relationship between precision-recall and roc curves," in *Proceedings of the 23rd international conference on Machine learning*, 2006, pp. 233–240.
- [59] S. Rajapaksha, G. Madzudzo, H. Kalutarage, A. Petrovski, and M. O. Al-Kadri, "CAN-MIRGU: A Comprehensive CAN Bus Attack Dataset from Moving Vehicles for Intrusion Detection System Evaluation," in *Symposium on Vehicles Security and Privacy*. Internet Society, 2024. [Online]. Available: <https://dx.doi.org/10.14722/vehiclesec.2024.23043>



Pablo Moriano (Senior Member, IEEE) received B.S. and M.S. degrees in electrical engineering from Pontificia Universidad Javeriana in Colombia and M.S. and Ph.D. degrees in informatics from Indiana University Bloomington, Bloomington, IN, USA. He is a research scientist with the Computer Science and Mathematics Division at Oak Ridge National Laboratory, Oak Ridge, TN, USA. His research lies at the intersection of data science, network science, and cybersecurity. In particular, he uses data-driven and computational methods to discover, understand, and detect anomalous behavior in large-scale networked systems. Applications of his research range across multiple disciplines, including, the detection of exceptional events in social media, Internet route hijacking, insider threat behavior in version control systems, and anomaly detection in cyber-physical systems. Dr. Moriano is a member of ACM and SIAM.



Steven C. Hespeler earned his Bachelor's degree in Engineering with a minor in Mathematics from Roger Williams University, Bristol, RI, USA. Following his BS he completed a Master's degree in Industrial Engineering and Ph.D. in Industrial Engineering with a minor in Applied Statistics both from from New Mexico State University, Las Cruces, NM, USA. He is a Post-doctoral Research Associate with the Computer Science and Mathematics Division, Oak Ridge National Laboratory, Oak Ridge, TN, USA. His

research interests are a fusion of data science, non-destructive evaluation, and advanced signal processing. He has an overall research goal of enabling smart and interconnected systems and develops data-driven models with Machine/Deep Learning techniques for solving complex engineering challenges. The applications of his research encompass in-situ process monitoring and anomaly/defect detection within additive manufacturing, cybersecurity, and robotic inspection.



Mingyan Li is a Senior cybersecurity researcher at Oak Ridge National Laboratory (ORNL). She joined ORNL in 2021, after working at Boeing Research and Technology for 15 years. She received a Ph.D. in EE from University of Washington. Her research interests include cybersecurity data analytics, AI-based IoT/cloud system security/privacy, and key management; within and beyond distributed computing and transportation system domains.



Robert A. Bridges is a Senior Research Mathematician at ORNL sitting in the National Security Sciences Directorate. Bobby currently focuses on advancing differentially private machine learning and using mathematical system models to identify feedback vulnerabilities. Bobby holds an undergraduate degree from Creighton University in mathematics as well as a PhD in mathematics from Purdue University. Leaving pure mathematics, Bobby was fortunate to obtain a postdoc position at ORNL in 2012,

where he has since supported a wide variety of projects with machine learning, statistical, and applied math expertise. Previous work includes leading projects on intra-vehicle network security and reverse engineering algorithms, leading large-scale experiments testing commercial security tools, and serving for 2 years as the Cybersecurity Research Group Leader.